K-Band Quasi-Planar Tapped Combline Filter and Diplexer

Wen-Teng Lo, *Student Member, IEEE,* and Ching-Kuang C. Tzuang, *Senior Member, IEEE*

***Abstract*—The quasi-planar realizations of combline bandpass filter and diplexer using multiple coupled suspended substrate striplines (MCSSS's) have demonstrated good performance at K-band without any tuning. The N MCSSS's excite N zero-cutoff-frequency quasi-TEM modes. A new computer-aided filter design approach employing rigorous SDA (spectral-domain-approach) and $2N$-port microwave circuit theory accounts for the effects of the N quasi-TEM modes, the couplings through non-adjacent MCSSS's, and cover height. Two 19.5-to-20.5 GHz MCSSS's combline filters with different cover heights are built and tested to compare their filter characteristics. The reduction in cover height decreases the amount of non-adjacent couplings through MCSSS's and results in better filter stopband performance. Another 18.5-to-19 GHz and 20-to-20.5 GHz MCSSS's diplexer is also presented. All the measured results for the combline filters and diplexer agree well with the theoretic calculations.**

I. Introduction

RECENT advances in millimeter-wave receiver technology has created a great demand for small, compact, low-cost and high-performance filters, diplexers, and multiplexers, which are commensurate with (M)MIC technologies. Conventional combline filter, in particular, features compact in size, very steep cutoff rate near the high side of the passband, good and broad stopband performance, and ease of fabrication tolerance [1]–[3]. Furthermore, the tapped-line arrangement makes the combline filter even more compact and easy to interface with other circuit components [4], [5]. With all these merits the combline filter had been widely used in RF communication equipments.

The conventional combline filter consists of a set of parallel metal bars loaded the lumped capacitors made of tuning screws. When designing a combline filter approaching millimeter-wave frequency (30–300 GHz), the conventional filter becomes too small to fabricate and adjust. For example, the dimensions of an L-band (1.2-to-1.8 GHz) three-resonator metal bars combline filter [3], with 27.5° electric length in the center of passband, are about 19.86 mm by 15.28 mm. By linearly scaling down the filter from L-band into X-band (8-to-12 GHz) and K-band (18-to-26.5 GHz), the overall physical dimensions will be about 19.86 mm by 2.29 mm and 19.86 mm by 1.03 mm, respectively. Within such small area, for placing resonators and tuning elements, great engineering design efforts and cares must be exercised to build the scaled-down filters. Thus an alternative way of realizing combline filter is needed.

By using the susceptance-annulling network, combline bandpass filters can be further connected together at a common junction to form a diplexer or a multiplexer [6]–[9]. This allows filtering for the different signal channels under a variety of applications such as telemetry and electronic warfare. The conventional filter consists of inductive array of rods mounted on a common surface. The large number of resonators can be tuned by adjusting the screws associated with the filter.

The miniaturization of the conventional metal bars combline filter or multiplexer operating at higher frequencies increases the complexity in handling the mechanical tooling of such filters. The filter adjustment becomes increasingly difficult because the dimensions of the tuning screws are much smaller to work with. To avoid these difficulties, quasi-planar transmission lines, replacing the air-filled coaxial lines and parallel-coupled lines, are proposed to take full advantage of all the merits of combline filter and make it (M)MIC integrable. This paper presents a feasibility study together with experimental proofs of designing combline filters using the quasi-planar multiple coupled suspended substrate striplines (MCSSS's) without requiring any tuning adjustment. The challenge here is common to MMIC (monolithic microwave integrated circuits) chip designers attempting to achieve first-pass success, which is also closely related to the so-called producibility engineering of MMIC's [10], [11].

Figs. 1 and 2 illustrate the three-dimensional view of the experimental MCSSS's combline bandpass filter and diplexer, respectively. Except the metallic housing requiring the precision tooling, the MCSSS's configurations require two masks, which can be easily adopted into conventional (M)MIC photolithography process. In Fig. 1, the conventional parallel metal bars now become the MCSSS's grounded on the same side. The tuning capacitors are replaced by the MIM (metal-insulator-metal) capacitors, which have much higher Q-factors than those of beam-lead capacitors used in the previously reported microstrip realization of combline filter [12]. Fig. 2 shows a susceptance-annulling version of a combline diplexer. The filter configurations shown in Figs. 1 and 2 can directly link themselves to other (M)MIC components without being modulized.

It seems, at the first glance, that the proposed quasi-planar versions are simply one-to-one replacement of the conventional metal bars designs. They differ, however, by one major guided-wave property. Namely, the quasi-planar real-

Manuscript received January 13, 1992; revised May 1, 1992. This work was supported by the National Science Council, R.O.C., in part under Grant NSC81-0404-E009-120 and in part under Contract CS82-0210-D006-026.

The authors are with the Institute of Electrical Communication Engineering National Chiao Tung University No. 1001, Ta Hsueh Road, Hsinchu, Taiwan, R.O.C.

IEEE Log Number 9204474.

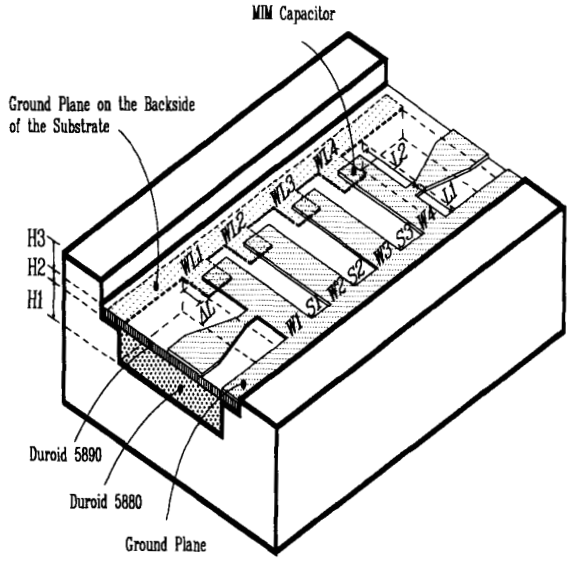

Fig. 1. The three-dimensional view of the new MCSSS's combline filter configuration with the top cover taken off. The structural parameters are listed in Table I.

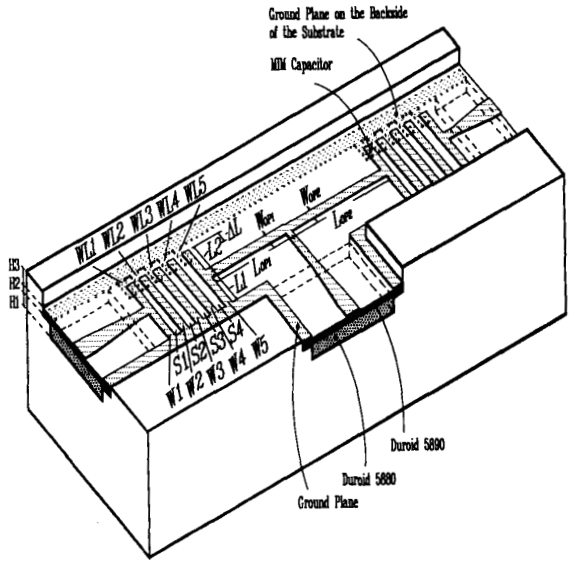

Fig. 2. The three-dimensional view of the proposed combline diplexer configuration with the top cover taken off. The structural parameters are listed in Table II.

TABLE I
THE STRUCTURAL PARAMETERS OF THE TWO TESTED MCSSS'S COMBLINE BANDPASS FILTERS WITH DIFFERENT COVER HEIGHTS

UNIT: MIL	FILTER 1	FILTER 2
W1=W4	14.70	11.45
W2=W3	14.70	11.50
WL1=WL4	14.70	11.45
WL2=WL3	14.70	11.50
S1=S3	12.20	10.40
S2	31.00	21.70
ΔL1=ΔL4	12.00	15.10
ΔL2=ΔL3	12.30	15.00
L1	38.00	36.00
L2	46.60	46.00
C1=C4	0.053 pF	0.055 pF
C2=C3	0.055 pF	0.055 pF
H1	10.00 (εr = 1 or 2.2*)	
H2	2.00 (εr = 2.1**)	
H3	100.00 (εr = 1)	30.00 (εr = 1)

*: Duroid 5880 **: Duroid 5890

TABLE II
THE STRUCTURAL PARAMETERS OF THE EXPERIMENTAL MCSSS'S COMBLINE DIPLEXER

UNIT: MIL	CHANNEL 1	CHANNEL 2
W1=W5	14.21	14.30
W2=W4	14.49	14.09
W3	14.49	14.01
WL1=WL5	14.21	14.30
WL2=WL4	14.49	14.09
WL3	14.49	14.01
S1=S4	6.01	7.48
S2=S3	22.25	21.87
ΔL1=ΔL5	12.00	12.50
ΔL2=ΔL4	14.00	11.00
ΔL3	14.00	11.00
L1	43.10	43.14
L2	51.18	51.02
Wop	24.00	24.00
Lop	272.0	297.0
C1=C5	0.047 pF	0.051 pF
C2=C4	0.056 pF	0.044 pF
C3	0.056 pF	0.043 pF
H1	10.00 (εr = 1 or 2.2*)	
H2	2.00 (εr = 2.1**)	
H3	30.00 (εr = 1)	

*: Duroid 5880 **: Duroid 5890

izations support N zero-cutoff-frequencies quasi-TEM modes in addition to all other higher-order modes possibly excited. Using Fig. 1 as an example, four MCSSS's will result in four quasi-TEM modes with different propagation constants. All the classical design approaches [1]–[5], assuming one degenerate single-valued propagation constant in the conventional air-filled combline filters, can't accurately design the quasi-planar version with prescribed filter characteristics.

The second critical issue associated with the new design approach is the fact that other than adjacent coupling between the resonators (MCSSS's), e.g., between the first resonator and the third resonator, becomes a serious problem when the filter dimensions are getting smaller. It can be shown that if the dielectric medium is inhomogeneous the importance of couplings beyond nearest neighbor lines becomes more significant, and they are quite significant in the structures treated in this paper. Again, all the classical design approaches [1]–[5] neglect these effects.

The third issue is how to design accurately the MIM capacitors used in the new filter configurations. On the opposite side of the MCSSS's, a toothed metalization pattern is formed right under the corresponding MCSSS's. Since the (M)MIC photolithography technique can easily achieve the tolerance less than 0.5 mil, the values of lumped capacitors can be accurately controlled. This will result in highly reproducible (M)MIC combline filters.

The three critical issues mentioned above require one thing in common, i.e., accurate field-theoretic analysis of the complicated geometry as depicted in Figs. 1 and 2. Instead of applying the inapplicable exact filter synthesis theory, which assumes one degenerate single-valued propagation constant and zero non-adjacent couplings between resonators [3],

this paper adopts the modified Newton optimization algorithm incorporating the combined used of the two-dimensional and three-dimensional quasi-static spectral-domain analyses of MCSSS's and MIM capacitors with the updated layout parameters. Section II-A describes the field-theoretic analysis of the N MCSSS's that result in a $2N$-port microwave circuit for use in the CAD (computer-aided-design) of the filters. Section II-B shows how the MIM capacitors can be designed using the three-dimensional SDA (Spectral Domain Approach) coupled with a deembedding process. Section III describes the design of the MCSSS's tapped combline filter both theoretically and experimentally. A simple technique to decrease the effects of the non-adjacent coupling using MCSSS's is described. As a result, the stopband performance is improved in one of the two tested filters. Section IV presents the susceptance-annulling type of diplexer connected by two channel filters designed in the same way as described in Section III. All the experimental filters require no tuning to achieve the desired passband characteristics.

II. $2N$-Port Microwave Circuit for the MCSSS's

Fig. 3 shows the schematic drawing of a tapped combline bandpass filter used to derive the corresponding 2-port S parameters. The N parallel-coupled lines are divided into two regions, which have the lengths of L_1 and L_2 and the associated $2N$-port admittance matrices are $[Y_{2N}]_{L1}$ and $[Y_{2N}]_{L2}$, respectively. The lower region has the common ground on the same side. The other one is loaded with the lumped capacitors denoted by $[jB]_c$. Here the T-junction at the input and output tapped lines uses the same model as shown in [13]. By imposing the appropriate terminating conditions, the two $2N$-port circuits are reduced to a 2-port circuit. It is a straightforward process and will not be repeated here [14, ch. 11]. The tapped MCSSS's combline diplexer is designed in a similar way. Two MCSSS's tapped combline bandpass filters are designed first and then the susceptance-annulling networks are determined. The whole circuits are then tied together to form a final 3-port circuit. Note that the derived circuit parameters take into account the effects of the multiple quasi-TEM modes, the non-adjacent couplings between coupled lines, and the cover height.

The spectral domain approach (SDA) is adopted for analyzing the physical layout associated with Fig. 3. The two-dimensional SDA is used to obtain the $2N$-port circuit parameters and the three-dimensional SDA is used to calculate the values of MIM capacitors. The discontinuity parameters near the junctions of the MIM capacitors are obtained by the combined uses of two-dimensional and three-dimensional SDA.

A. Derivation of $2N$-Port Circuit Parameters Based onTwo-Dimensional SDA

Consider a system of striplines in a stratified lossless dielectric region enclosed by conducting walls. Conductors can be coplanar or non-coplanar strips. To obtain quasi-TEM mode, the static potential distribution $\Phi(x, y)$ in the coupled

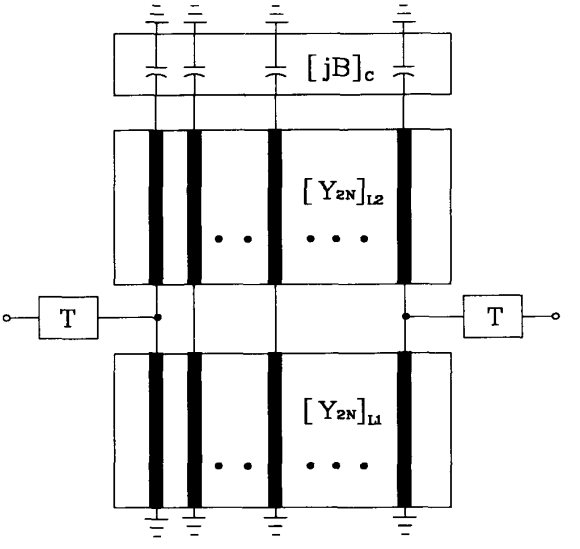

Fig. 3. The schematic drawing of a tapped combline filter used to derived the 2-port S parameters.

planar or quasi-planar structure satisfies the Poisson's equation

$$\nabla^2\Phi(x,y) = -\rho(x,y)/\varepsilon \tag{1}$$

and the boundary conditions on the surface of the dielectric material and the conductors. Here $\rho(x, y)$ is the charge distribution on the surface of the conducting strips. Instead of solving the two-dimensional partial differential equation in the space domain, we will work in the Fourier transform domain (FTD). Define the Fourier transform of $\Phi(x, y)$ as

$$\begin{aligned}\tilde{\Phi}(\alpha_p, y) &= \mathcal{F}\{\Phi(x,y)\} \\ &= \frac{2}{L}\int_0^L \Phi(x,y)\sin(\alpha_p x)\,dx\end{aligned} \tag{2}$$

where L is the distance between the two conducting walls along the x axis and $\alpha_p = p\pi/L, p = 1, 2, \cdots, P$. Taking the Fourier transforms on both sides of (1), we obtain

$$\left[-\alpha_p^2 + \frac{\partial^2}{\partial y^2}\right]\tilde{\Phi}(\alpha_p, y) = -\frac{1}{\varepsilon}\tilde{\rho}(\alpha_p, y). \tag{3}$$

By imposing the bounding conditions in solving (3), one obtains a set of linear inhomogeneous equations for the potential functions in each region. This leads to the determination of the dyadic Green's functions in the Fourier transform domain [15], [16, ch. 5].

In the SDA, the unknown charge density distribution $\rho(x, y)$ is expanded by a set of basis functions. The choice for such basis functions should comply with the assumption that the strips are infinitely thin perfect conductors. Since the quasi-TEM SDA is adopted, the strip currents have the longitudinal component only. Leaving out the transverse current components in the full-wave SDA [17], [18], one obtains the following expression for the ith charge-density distribution

$\rho_i(x,y)$ for the ith strip either at $y = H_1$, or $y = H_1 + H_2$:

$$\rho_i(x,y) = \sum_{m=1}^{M} A_{im}\rho_{im}(x,y) + \sum_{m=1}^{M} B_{im}\xi_{im}(x,y) \quad (4a)$$

$$\rho_{im}(x,y) = [1-u]^{(m-2)/2} - \sqrt{2}[1-u]^{(m-1)/2} + 0.5[1-u]^{(m/2)} \quad (4b)$$

$$\xi_{im}(x,y) = [1+u]^{(m-2)/2} - \sqrt{2}[1+u]^{(m-1)/2} + 0.5[1+u]^{m/2} \quad (4c)$$

where $u = 2(x - x_i)/w_i, x_i$ and w_i are the x-component of the center point and the width of the ith conductor strip, respectively. Followed by the well-known Galerkin's procedure and the application of the Parseval's theorem, the unknown coefficients $A_{im}, B_{im}, m = 1, \cdots, M$, and $i = 1, \cdots, N$, are solved. N is the number of conductor strips. Once $\rho_i(x,y)$ is known, the line capacitance C_{ij}(F/m) can be calculated from the variational expression [19]

$$\frac{1}{C_{ij}} = \frac{\oint \Phi(x,y)\rho_j(x,y)\,dx}{\oint \rho_1(x,y)\,dx \oint \rho_1(x,y)\,dx}. \quad (5)$$

The $2N$-port circuit parameters can be obtained from $[C_{ij}]$ as follows. We can obtain two capacitance matrices $[C]$ and $[C_0]$ with and without dielectric fills, respectively. Let $[A] = [C_0]^{-1}[C]$. The eigenvalues of $[A]$ are $\lambda_n, n = 1, 2, \cdots, N$. The eigenvectors of $[A]$ constitute the matrix $[M]$. Here the eigenvalues $\lambda_n, n = 1, 2, \cdots, N$, are the effective dielectric constants, which correspond to the various dominant quasi-TEM modes of the N parallel-coupled lines. The characteristic admittance matrix $[Y]$ of the N MCSSS's and the corresponding $2N$-port matrix $[Y_{2N}]$ can then be derived as [20]

$$[Y] = V_c[[M]^T]^{-1}[1/\sqrt{\lambda_n}]_{\text{diag}}[M]^T[C] \quad (6)$$

$$[Y_{2N}] = \begin{bmatrix} [Ya] & [Yb] \\ [Yb] & [Ya] \end{bmatrix} \quad (7a)$$

$$[Ya] = [Y][M][\coth(j\beta_n l_e)]_{\text{diag}}[M]^{-1} \quad (7b)$$

$$[Yb] = [Y][M][-\text{csch}(j\beta_n l_e)]_{\text{diag}}[M]^{-1} \quad (7c)$$

where $V_c(= 3 \times 10^8$ m/s) is the free space light velocity and $\beta_n(= \omega\sqrt{\lambda_n}/V_c)$ is the propagation constant for the nth dominant mode. The lengths of the N parallel-coupled lines are all equal to l_e. $[Ya]$ and $[Yb]$ are the self and mutual admittance matrices of the $2N$ port network, respectively.

Note that the characteristic admittance matrix $[Y]$ expressed in (6) includes all the multiple dominant modes and the couplings between adjacent and non-adjacent lines. If the N parallel coupled lines are placed in a homogeneous medium, the N multiple dominant modes have a degenerate single-valued propagation constant of $\beta(= \omega\sqrt{\lambda}/V_c)$. The characteristic admittance matrix reduces to

$$[Y] = (V_c/\sqrt{\lambda})[C]. \quad (8)$$

Equation (8) relates the characteristic admittance matrix $[Y]$ and the line capacitance matrix $[C]$ in a parallel-coupled transmission lines network when a degenerate single-valued propagation constant exists in the N parallel-coupled lines homogeneously-filled.

Applying the basis functions shown in (4), very accurate solutions for $[C]$ and $[C_0]$ can be obtained by setting $M = 3$ and $P = 400$ in (4) and (3), respectively. On the IBM RISC System/6000(model 320) workstation, the CPU time for obtaining a $[C]_{4\times4}$ matrix is approximately 1.56 seconds for a certain geometry of MCSSS's. This is short enough to be incorporated in the computer-aided design of quasi-planar combline filter and diplexer to be described later.

B. Deembedding the Discontinuity Parameters near the Junctions of MIM Capacitors by the Combined Use of Two-Dimensional and Three-Dimensional SDA

Accurate MIM capacitor model is as equally important as accurate $2N$-port Y-matrix for designing MCSSS's combline filter requiring no tuning adjustments. The fringing fields of the MIM capacitors realized by broadside coupled MCSSS's must be considered simultaneously. The accurate model for the system of MIM capacitors shown in Figs. 1 or 2 can be obtained by the three-dimensional SDA [21], which is essentially, in every aspect, parallel to what have been described in Section II-A and will not be repeated here.

The fringing fields of the MIM capacitors are often related to the open-end effective lengths [22] except that there are multiple lines in the present study. The discontinuity parameters at the junctions of the MIM capacitors and the open-circuited MCSSS's can be obtained by manipulating the various capacitance matrices. Assuming that there are N MCSSS's and N MIM capacitors. For the sake of clarity, we number the N MCSSS's from 1 to N and the corresponding N MIM capacitors from $N + 1$ to $2N$. The three N by 1 column vectors $\boldsymbol{A}, \boldsymbol{B}$, and $\boldsymbol{C}$ are defined as follows.

- $\boldsymbol{A} = [a_i]$ $a_i = \Sigma_{j=1}^{N} C_{a(i),(j)} = c_{0(i)}$ for $i = 1, \cdots, N$. The capacitance matrix $[C_{a(i),(j)}]_{N\times N}$ is computed by the two-dimensional SDA program for the N MCSSS's of infinite length. Thus a_i is the self capacitance per unit length of $c_{0(i)}$(F/m) of ith uniform MCSSS with respect to the ground potential.
- $\boldsymbol{B} = [b_i]$ $b_i = \Sigma_{j=1}^{N} C_{b(i),(j)} = 2l_e c_{0(i)} + 2c_{f(i)}$ for $i = 1, \cdots, N$. The capacitance matrix $[C_{b(i),(j)}]_{N\times N}$ is computed by the three-dimensional SDA program for the N MCSSS's of length $2l_e$. Thus b_i is the ith self capacitance (F), consisting of uniform line capacitance of $2l_e c_{0(i)}$ and two open-end fringing field capacitance of $2c_{f(i)}$ at the two open-end sides.
- $\boldsymbol{C} = [c_i]$ $c_i = \Sigma_{j=1}^{2N} C_{c(i),(j)} = l_e c_{0(i)} + c_{fe(i)} + c_{f(i)}$ for $i = 1, \cdots, N$. The capacitance matrix $[C_{c(i),(j)}]_{2N\times2N}$ is computed by the three-dimensional SDA program for the N MCSSS's of length l_e and the N MIM capacitors. Thus c_i is the self capacitance (F) of the ith MCSSS with respect to the ground

potential. The capacitance c_i consists of uniform line capacitance of $l_e c_{0(i)}$, one open-end fringing field capacitance of $c_{fe(i)}$ near the MIM capacitor, and one open-end fringing field capacitance of $c_{f(i)}$ far from the MIM capacitor. Here, the coupling capacitance $C_{c(i),(N+i)}$ is the amount for the ith MIM capacitor.

The open-end effective length near the MIM capacitors is then given by

$$\Delta_i = (c_i - b_i/2)/a_i = c_{fe(i)}/c_{0(i)} \qquad i = 1, \cdots, N. \quad (9)$$

In general, depending on the amount of the overlapped area for the MIM capacitors as shown in Figs. 1 or 2, the values of Δ_i can be a positive or negative in values [21], [23]. The lengths of MCSSS's should be compensated by Δ_i to obtain the correct electrical lengths for the desired filter performance.

III. MCSSS's Realization of Tapped Combline Bandpass Filter

A. The Iterative Method of Designing a MCSSS's Tapped Combline Filter

To design the tapped MCSSS's combline filter, a new design approach is necessary because the exact equivalent circuit of the tapped MCSSS's combline filter is too complicated to be synthesized when considering the presences of the multiple quasi-TEM modes and the non-adjacent couplings between the resonators. While the conventional approximate [1], [2], [4], [5] or exact [3] filter synthesis techniques can not apply to the MCSSS's combline filter designs, a computer iterative design approach is adopted. Initially we assume that there exists one degenerate single-valued propagation constant and neglect the non-adjacent couplings between resonators. The tapped line model [5] and the exact filter synthesis [3] for combline filter are invoked under these assumptions for obtaining the starting design. Assuming that the length of the commensurate combline filter is L. The tapped line equivalent circuit is approximated by adding one unit element of length L', which only adds to extra phase delay of the original filter, at each end of the two-port of a commensurate combline filter. By successively applying the Norton transformation and Kuroda's identity one can obtain the equivalent circuit of a tapped combline filter with the tapped point, measured from the common ground end, at $L_T (L_T = L - L')$. The circuit parameters are then transferred to the physical dimensions $(W_1, S_1, W_2, S_2, \cdots$ of Fig. 1) by an optimization routine. This is done by matching y_{ij} of Fig. 4 in [5] to the tridiagonal terms of (6) of this paper. Up to now the starting design for the iterative solution of the final filter geometry is established. To obtain the desired filter performance we use another optimization routine by fine tuning the physical dimensions obtained from the starting design. The layout adjustment is based on the two-dimensional and three-dimensional SDA approaches described in Section II. Therefore the composite effects of the multiple quasi-TEM modes, the non-adjacent couplings between MCSSS's, and the cover height are all considered simultaneously. Furthermore, we can use this optimization routine to adjust the length of resonator to give the lumped capacitor at a resonable value for realization. The capacitance values as well as the discontinuity parameters at the junction of MCSSS's and MIM capacitors are then determined using the method described in Section II-B.

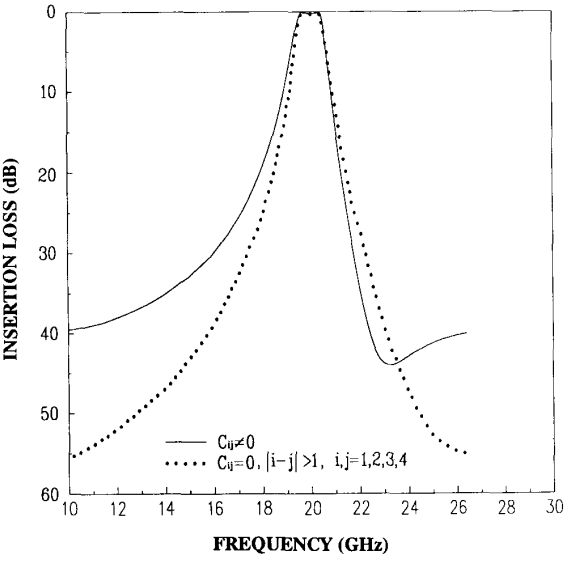

Fig. 4. Theoretic results for indicating the effect of non-adjacent couplings between MCSSS's.

B. The Effect of Non-Adjacent Couplings Between the Resonators of MCSSS's Combline Filter

Using the method described previously, a four-resonator tapped combline bandpass filter centered at 20 GHz with 5 percent fractional bandwidth is designed. The calculated theoretic results are shown in Fig. 4. The CAD approach allows us to switch the program between two modes. One considers only the adjacent couplings among the MCSSS's and the other includes all the couplings. When $C_{ij} \neq 0$ for all $i, j = 1, 2, 3, 4$, the calculated insertion loss is shown under solid line. When we set $C_{ij} = 0$ for all $|i - j| > 1, i, j = 1, 2, 3, 4$, the stopband performance as shown under dotted line can be improved. In Fig. 4 the stopband performance is improved by about 15 dB at 10 GHz for this particular case. It is also found that, by reducing the cover height, the non-adjacent couplings between MCSSS's can be reduced. This suggests a way to design the MCSSS's combline filter with improved stopband performance without increasing the number of resonators. Such finding is important for not using excessive number of resonators that will introduce the undesired passband losses to achieve a better stopband performance.

C. MCSSS's Combline Filter Design Examples

In Fig. 1 the dashed lines region near the input port and output port, a Duroid 5880 (10 mils, $\varepsilon r = 2.2$) substrate is inserted below the Duroid 5890 (2 mils, $\varepsilon r = 2.1$) substrate and an optimum Chebyshev type taper is built on it [24], [25]. The input port and output port are tapered from 50 Ω to 75 Ω,

which is the filter's internal normalized impedance. There are two main reasons to make such arrangement. The first is to reduce the width of the input (output) line which is connected to the first (last) resonator line of the filter. Otherwise the dimension of the T-junctions formed at the tapped position can be close to the length of MCSSS's. For example, the width of a 50 Ω line is about 50 mils under current configuration. Compared to the length of MCSSS's, 84.6 mils in the present study, the T-junction is too big to realize. The second reason is to have a better transition from the coaxial line to the microstrip line on top of the Duroid 5880 substrate as shown in Figs. 1 or 2. At the end of each resonator line, a high-Q MIM capacitor is used.

Two 19.5 to 20.5 GHz bandpass prototypes with different cover heights are built and tested. The passband ripples are assumed to be 0.2 dB for these two prototypes. The structural parameters are listed in Table I. Note that the structural parameters need modifications to have the same passband performance when the cover height changes. Filter 1 has cover height of 100 mils and filter 2 has cover height of 30 mils. Both theoretic and measured insertion losses and return losses are shown in Fig. 5(a) and (b), respectively. The measured insertion losses for the two prototypes are about 1.2 dB. As can be seen that the stopband performance is indeed improved to a considerable extent when the cover height is reduced from 100 mils to 30 mils. The deviations between theoretic and measured results in the high side of the stopband and in the lower side of the stopband at approximately 11 GHz for both prototypes are probably due to the excitations of the higher order modes. When looking into the direction parallels to that of MCSSS's, the dimensions of the cross section should include the two long tapered-line sections and the filter itself. Our SDA program shows that there are two additional higher-order modes possibly excited in addition to the four dominant quasi-TEM modes. One of the two higher-order modes has a cutoff frequency at 10.30 GHz and the other at 20.54 GHz.

In these two examples, the propagation constants of the multiple quasi-TEM modes associated with the MCSSS's are approximately equal to each other, so the improvement in the stopband performance as compared to what had been reported previously in [12] is mainly due to the reduction in the non-adjacent couplings between MCSSS's. The tapped line arrangement at the input and output ends and the use of lumped capacitors destroy the periodic property of the commensurate linelength. The first spurious response is found to occur at about 75 GHz for these two prototypes.

Fig. 6 is the photograph of the two prototypes. The complete circuit is printed on a single substrate. This makes it reproducible since photolithography technique can easily manage the tolerance requirement required for making such circuit. Both filters feature 14.4 mm by 2.5 mm in size including the tapered sections. These tapered sections occupy most of the space in the filter. In practical applications, however, the filter does not need to be connected to a 50 Ω line. Without these tapers the filter dimensions are about 3.0 mm by 2.5 mm. For frequency goes above 40 GHz, the dimensions of the MCSSS's combline filter will be less than 1 mm by 1 mm. This makes the MCSSS's combline filter an attractive choice

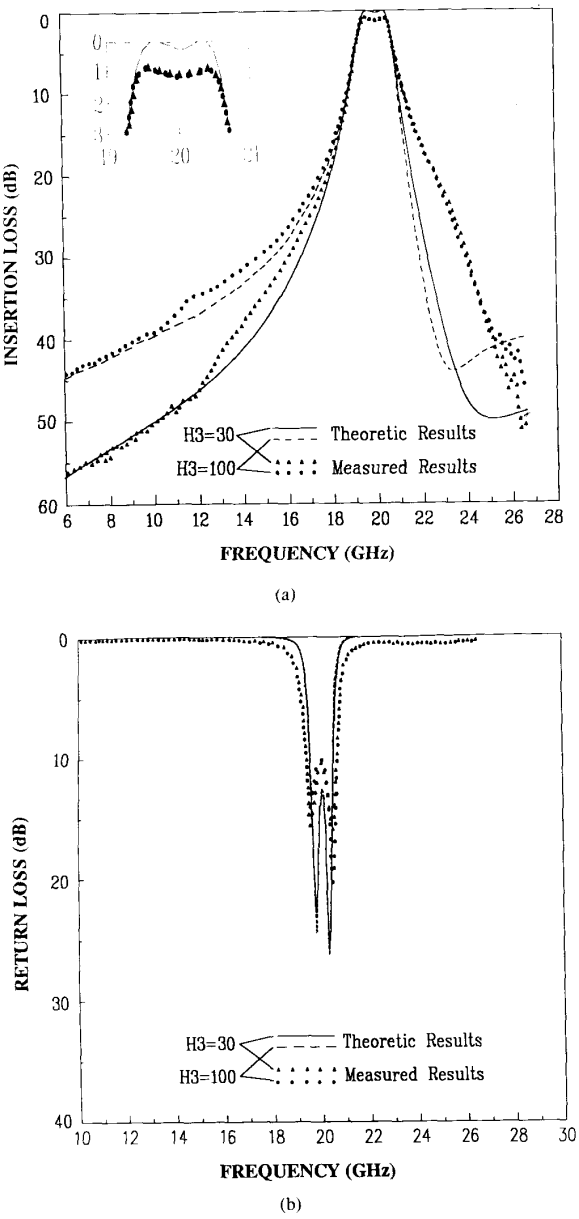

Fig. 5. Theoretic and measured results of the two tested tapped combline filters having different cover heights. (a) Insertion loss. (b) Return loss.

for use in (M)MIC's. Furthermore, the line widths W_1, W_2, etc. are limited by the minimum geometry and skin depths in the MMIC technologies. Thus a further reduction from about 14 mils to 1 mil for the line width is possible if MMIC process is adopted.

D. Theoretic Q of a Combline Filter Using MIM Capacitor

The theoretic unloaded quality factor Q_u of a single resonator of MCSSS's combline filter associated with Fig. 1 can be computed as follows. Considering the 2nd resonator of filter 1 or filter 2, for example, the quality factor Q_c of

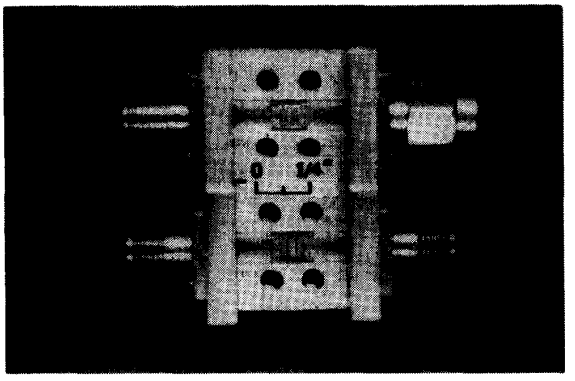

Fig. 6. Photograph of the prototype of the tapped combline filters.

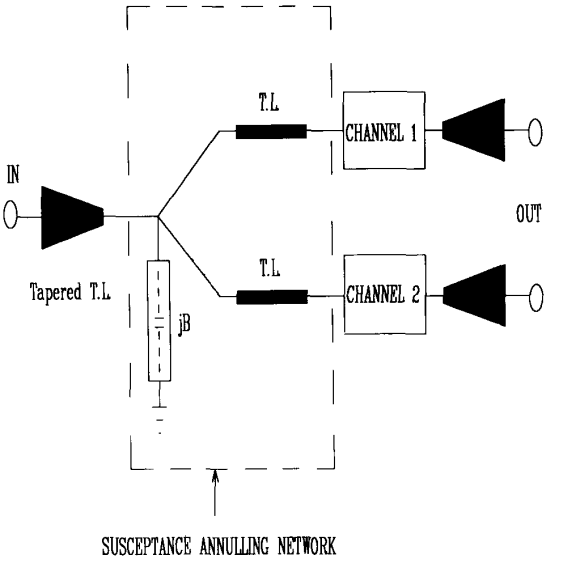

Fig. 7. Schematic drawing of a parallel-connected diplexer.

MIM capacitor using the Duroid 5890 ($\tan\delta \approx 0.0009$. at 20 GHz) is about 900 at 20 GHz [14, ch. 7]. The α/β is computed to be 9.412×10^{-4} and 9.758×10^{-4} for filter 1 and filter 2, respectively, where α is the attenuation in nepers per meter and β is the phase constant of the transmission line at resonant frequency. Then the theoretic Q_u of a suspended substrate stripline resonator loaded with the MIM capacitor can be obtained from (1) of [2]. The theoretic Q_u is approximately 500 for filter 1 and 490 for filter 2. Some factors, such as the surface roughness of the metal strip, imperfect mechanical contact between ground and resonator line, etc., will further reduce the value of Q_u. For the two tested prototypes, the dB increase in attenuation at the center frequency of the passband is about 1.0 dB. According to (4.13–8) and Fig. 4.13–2 of [26], the measured Q_u of a single resonator for the MCSSS's combline filter is approximately 422.

IV. MCSSS's Realization of the Tapped Combline Diplexer

Fig. 7 shows the schmatic drawing of a parallel-connected diplexer. The susceptance-annulling network is added to help preventing the two channel filters from interacting across the operating bands. The susceptance-annulling network, enclosed by the dashed line in Fig. 7, is similar to that introduced by LaTourrette [7]–[9]. It is incorporated here to design the MCSSS's tapped combline diplexer. Thus the susceptance annulling network consists of two transmission lines (TL's) and a capacitor connected to the common junction. The TL's separate the two filters physically and act as immittance compensation network. An optimization process is used again by varying the lengths (L_{OP1}, L_{OP2}) and the characteristic impedances (the widths W_{OP1}, W_{OP2}) of the TL's and the capacitance (jB) of the shunt capacitor to obtain a satisfactory design. In our particular design the capacitance is so small that it can be neglected for the prototype. Table II lists the optimized structural parameters corresponding to Fig. 2 showing the three-dimensional view of the MCSSS's diplexer.

In Fig. 2 the combline filters consist of five resonators. The two channel filters are designed to have 0.5 GHz bandwidth centered at 18.75 GHz and 20.25 GHz with passband ripples of 0.2 dB, respectively. Fig. 8(a) and (b) plot the theoretic and measured results of the insertion losses and return losses, respectively. Close agreements in these plots are obtained except that the passbands have approximately 1.7 dB losses. The resonance and the corresponding spikelike response at the lower side of the passband is due to the long transmission lines which have the effect of transforming the behavior of upper side of the passband. This can be avoided by using higher impedance and shorter length transmission lines as the compensation network. Again the excited higher-order modes in the direction parallel to the MCSSS's degrade the stopband performance. Fig. 9 is the photograph of the prototype of the tapped combline diplexer. The photolithography was kept to within ± 0.5 mils. No tuning adjustment was performed to obtain the measured results reported in Fig. 8(a) and (b).

The accurate values of the MIM capacitors are critical to obtain the correct response for designing the combline filter and/or diplexer using MIM capacitors. Some factors such as the uniformity of the substrate material, the thermal coefficient of dielectric constant and expansion of the substrate will change the values of the MIM capacitors. The simulated results show that the two passbands of the diplexer shift by about 2% for $\pm 0.5\%$ variation in substrate thickness. Similarly the two passbands shift downward and upward by approximately 8% of the passband bandwidth for 30°C-to-0°C and 30°C-to-100°C temperature variations, respectively. The temperature sensitivity is an important factor to be considered in the step of choosing substrate for designing the combline filter and/or diplexer using MIM capacitors.

V. Conclusion

A new design of MCSSS's tapped combline filter is presented. The quasi-planar realization of combline filters retains all the merits of the conventional metal-bar combline filters and makes them compatible with (M)MIC technologies. To obtain a predictable and controllable filter performance using

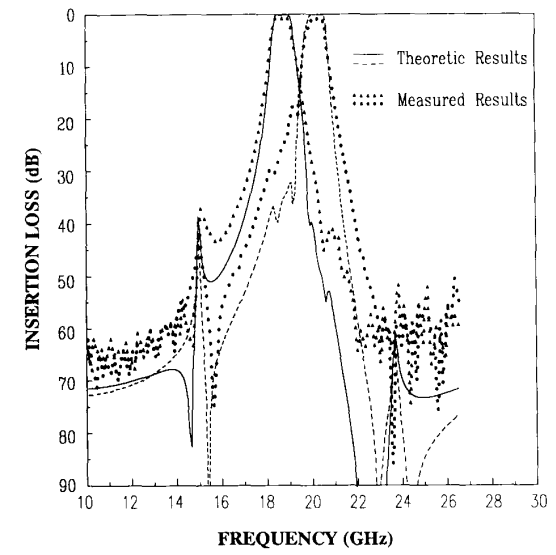

Fig. 8. The theoretic and measured results of the prototype tapped combline diplexer. (a) Insertion loss. (b) Return loss.

planar or quasi-planar transmission lines the composite effects of the multiple quasi-TEM modes, the non-adjacent couplings between MCSSS's, and the cover height must be considered at the same time. The use of iterative computer-aided design procedure that incorporates rigorous and fast field-theoretic analysis of the combline filter enables us to design the MCSSS's combline filter and diplexer without any tuning. An important feature of our approach is that the network structure is fully exploited thereby the composite effects mentioned above can be fully considered. This reduces the cost and labor of implementing such MCSSS's combline filter and diplexer by achieving the first-pass success as required by

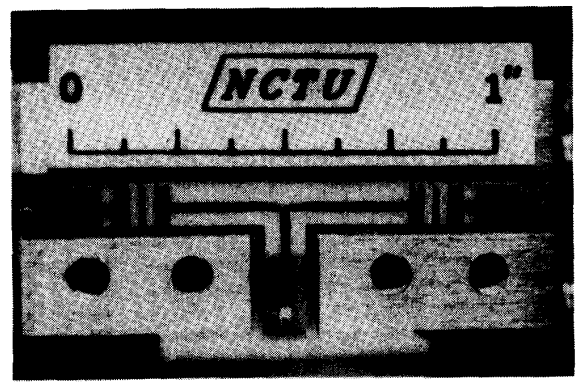

Fig. 9. Photograph of the prototype of the tapped combline diplexer.

MMIC technology. The measured and theoretic results for the combline filter and diplexer are in good agreements. The discrepancies occur in the stopband and passband are explained. The generation of higher-order modes parallel to the direction of MCSSS's should be avoided to improve the stopband performance. The unloaded Q_u of the filter is closely related to the passband losses. The presented MCSSS's combline filter realization can be a viable filter candidate for use in (M)MIC's.

ACKNOWLEDGMENT

The authors would like to thank Mr. C.-N. Lee for providing the two-dimensional SDA program and Mr. Y.-C. Chiang for the three-dimensional SDA program. Thanks are also due to Steve Cheng for his assistance with measurements. Special thanks also to the reviewer for his comments on the concept of degenerate TEM modes of the homogeneously-filled MCSSS's. We also quote his suggestion which appears in the last sentence of the seventh paragraph of the Introduction section. The comment on the temperature stability of the proposed filter structure by another reviewer is also warmly appreciated.

REFERENCES

[1] G. L. Matthaei, "Comb-line band-pass filters of narrow or moderate bandwidth," *Microwave J.*, vol. 6, pp. 82–91, Aug. 1963.
[2] E. G. Cristal, "Capacity coupling shortens comb-line filters," *Microwaves*, vol. 6, pp. 44–50, Dec. 1967.
[3] R. J. Wenzel, "Synthesis of combline and capacitively loaded interdigital bandpass filters of arbitrary bandwidth," *IEEE Trans. Microwave Theory Tech.*, vol. MTT-19, no. 8, pp. 678–686, Aug. 1971.
[4] S. Wong, "Microstrip tapped-line filter design," *IEEE Trans. Microwave Theory Tech.*, vol. MTT-27, no. 1, pp. 44–50, Jan. 1979.
[5] E. G. Cristal, "Tapped-line coupled transmission lines with applications to interdigital and combline filter," *IEEE Trans. Microwave Theory Tech.*, vol. MTT-23, pp. 1007–1012, Dec. 1975.
[6] E. G. Cristal and G. L. Matthaei, "A technique for the design of multiplexers having contiguous channels," *IEEE Trans. Microwave Theory Tech.*, vol. MTT-12, pp. 88–93, Jan. 1964.
[7] P. M. LaTourrette, "Multi-octave combline-filter multiplexers," in *IEEE MTT-S, Int. Microwave Symp. Dig.*, 1977, pp. 298–301.
[8] ——, "Combline filter multiplexers," *Microwave J.*, vol. 20, no. 8, pp. 55–59, Aug. 1977.
[9] P. M. LaTourrette, and J. L. Roberds, "Extended-junction combline multiplexers," in *IEEE MTT-S, Int. Microwave Symp. Dig.*, 1978, pp. 214–216.

[10] A. K. Sharma, "Considerations in producibility engineering of MMIC's," *IEEE Trans. Microwave Theory Tech.*, vol. 38, pp. 1242–1248, Sept. 1990.
[11] R. H. Jansen, R. G. Arnold, and I. G. Eddison, "A comprehensive CAD approach to the design of MMIC's up to mm-wave frequencies," *IEEE Trans. Microwave Theory Tech.*, vol. 36, pp. 208–219, Feb. 1988.
[12] C.-K. C. Tzuang and W.-T. Lo, "Printed-circuit realization of a tapped combline band-pass filter," *IEEE MTT-S, Int. Microwave Symp. Dig.*, 1990, pp. 131–134.
[13] P. Silvester and P. Benedek, "Microstrip discontinuity capacitances for right-angle bends, T-junction and crossings," *IEEE Trans. Microwave Theory Tech.*, vol. MTT-21, no. 5, pp. 341–346, May 1973.
[14] K. C. Gupta, R. Gary, and R. Chadha, *Computer-Aided Design of Microwave Circuits*. Norwood, MA: Artech House, 1981.
[15] T. Itoh, "Generalized spectral domain method for multiconductor printed lines and its application to tunable suspended microstrips," *IEEE Trans. Microwave Theory Tech.*, vol. MTT-26, pp. 983–987, Dec. 1978.
[16] T. Itoh, *Numerical Techniques for Microwave and Millimeter-Wave Passive Structures*. New York: Wiley, 1989.
[17] C.-K. C. Tzuang and J.-T. Kuo, "Modal current distribution on closely coupled microstrip lines: A comparative study of the SDA basis functions," *Electron. Lett.*, vol. 26, no. 7, pp. 464–465, Mar. 29, 1990.
[18] J.-T. Kuo and C.-K. C. Tzuang, "Complex modes in shielded suspended coupled microstrip lines," *IEEE Trans. Microwave Theory Tech.*, vol. 38, pp. 1278–1286, Sept. 1990.
[19] R. E. Collin, *Field Theory of Guided Waves*, The Institute of Electrical and Electronics Engineers, pp. 277–279, 1991.
[20] D. Pompei, O. Benevello, and E. Rivier, "Parallel line microstrip filters in an inhomogeneous medium," *IEEE Trans. Microwave Theory Tech.*, vol. MTT-26, no. 4, pp. 231–238, Apr. 1978.
[21] C.-K. C. Tzuang, Y.-C. Chiang, and S. Su, "A compressed-length 90°-bent offset broad-side-end-coupled bandpass filter," *IEEE Microwave Guided Wave Lett.*, vol. 1, no. 10, pp. 285–287, Oct. 1991.
[22] R. S. Yahya, T. Itoh, and R. Mittra, "A spectral domain analysis for solving microstrip discontinuity problems," *IEEE Trans. Microwave Theory Tech.*, vol. MTT-22, pp. 372–378, Apr. 1974.
[23] C.-K. C. Tzuang, Y.-C. Chiang, and S. Su, "Design of a quasi-planar broadside end-coupled bandpass filters," *IEEE MTT-S, Int. Microwave Symp. Dig.*, 1990, pp. 407–410.
[24] R. W. Klopfenstein, "A transmission line taper of improved design," *Proc. IRE*, vol. 44, pp. 31–35, Jan. 1956.
[25] R. E. Collin, "The optimum tapered transmission line matching section," *Proc. IRE*, vol. 44, pp. 539–548, Apr. 1956.
[26] G. Matthaei, L. Young, and E. M. T. Jones, *Microwave Filters, Impedance-Matching Networks, and Coupling Structures*. New York: McGraw-Hill, 1964.

Ching-Kuang C. Tzuang (S'84–M'86–SM'92) was born in Taiwan on May 10, 1955. He received the B.S. degree in electronic engineering from the National Chiao Tung University, Hsinchu, Taiwan, in 1977 and the M.S. degree from the Univerity of California at Los Angeles in 1980.

From February 1981 to June 1984, he was with TRW, Redondo Beach, CA, working on analog and digital monolithic microwave integrated circuits. He received the Ph.D. degree in electrical engineering in 1986 from the University of Texas at Austin, where he worked on high-speed transient analyses of monolithic microwave integrated circuits. Since September 1986, he has been with the Institute of Communication Engineering, National Chiao Tung University, Hsinchu, Taiwan, R.O.C. His research activities involve the design and development of millimeter-wave and microwave active and passive circuits and the field theory analysis and design of various quasi-planar integrated circuits.

Wen-Teng Lo (S'90) was born in Taiwan on December 6, 1965. He received the B.S. degree in electronic engineering from the National Chiao Tung University, Hsinchu, Taiwan, in 1988. Since 1989, he has been working toward the Ph.D. degree at the same university. His current reseach interests include the analysis and design of microwave and millimeter-wave components.